Wear 274–275 (2012) 75–83

Contents lists available at ScienceDirect

Wear

journal homepage: www.elsevier.com/locate/wear

The effect of an alumina counterface on friction reduction of CuO/3Y-TZP composite at room temperature

Jiupeng Song[a,*], Mahdiar Valefi[a,*], Matthijn de Rooij[a], Dirk J. Schipper[a], Louis Winnubst[b]

[a] Surface Technology and Tribology Group, Faculty of Engineering, University of Twente, P.O. Box 217, 7500 AE Enschede, The Netherlands
[b] Inorganic Membrane Group, Faculty of Science and Technology and MESA+ Institute, University of Twente, P.O. Box 217, 7500 AE Enschede, The Netherlands

ARTICLE INFO

Article history:
Received 16 December 2010
Received in revised form 28 July 2011
Accepted 8 August 2011
Available online 27 August 2011

Keywords:
Ceramics
Composite
Sliding wear
Friction

ABSTRACT

The friction behavior of CuO/yttria-stabilized tetragonal zirconia (3Y-TZP) composite in dry sliding against alumina at room temperature has been investigated. The results show that an alumina counterface has a crucial role on the frictional behavior when sliding against CuO/3Y-TZP composite in comparison with other counter materials. Pure 3Y-TZP shows high friction and wear under the same conditions. It is found that the friction reduction behavior is dependent on the sliding test conditions such as load and humidity. A thin aluminum-rich layer less than 200 nm thick on the contact surface during the low friction situation has been found by various analyzing techniques including interference microscopy, micro-Fourier transform infrared spectroscopy (FTIR), X-ray photoelectron spectroscopy (XPS), scanning electron microcopy (SEM) and energy dispersive X-ray spectroscopy (EDX). The induced change of contact conditions and interfacial chemical reaction between CuO and alumina to form the phase $CuAlO_2$ increase the wear of alumina and accelerates the formation of an aluminum-rich surface layer. The presence of such a layer in the contact is beneficial for reducing friction. After a certain sliding distance, the coefficient of friction shifts from a low value to a high value due to a change in the dominating wear mechanism. This transition is shown to be caused by a different composition and thickness of the interfacial layer.

1. Introduction

Ceramics are used in applications due to their unique properties such as high hardness, low density, chemical inertness and the possibility of a high operational temperature in applications, like engines or turbines. However, the coefficient of friction for sliding ceramic couples is in general high. Further, it is not easy to use lubricants when ceramics are used at an elevated temperature. Ceramic composites containing a lubricating phase are desired to be developed to reduce friction. For example, the addition of graphite to the 3 mol% yttria-doped tetragonal zirconia (3Y-TZP) decreased the coefficient of friction from 0.56 to 0.29 during the dry sliding tests against GCr15 steel, but the wear rate increases rapidly when the graphite content was higher than a critical value [1]. Several solid oxide lubricants have been added to 3Y-TZP as second phase, but only CuO has shown the effect of reducing the coefficient of friction. The coefficient of friction of a 3Y-TZP disk sliding against alumina pin reduced from 0.70 to 0.43 by adding 5 wt.% CuO [2]. Pasaribu et al. [3] investigated the mild wear track with the low friction by nano indentation tests. The hardness of the polished surface of 3Y-TZP composite containing 5 wt.% CuO was 14 GPa, while the hardness inside the wear track reduced to 6 GPa. This indicates that there a rather soft surface layer is present in the wear track. This surface layer functions as a solid lubricant and reduces the coefficient of friction. Ran et al. [4] further studied this CuO/3Y-TZP composite and found that the sintering temperature and resulting ceramic microstructure had significant effect on the mechanical and tribological properties of CuO/3Y-TZP composite against alumina system. On the other hand, environmental effects on the frictional behavior of the CuO/3Y-TZP composite were also presented in previous work [5]. Nano tribological tests by atomic force microscopy (AFM) were also carried out on the above CuO/3Y-TZP systems [6]. The obtained coefficients of friction on nano scale were in agreement with the one from pin-on-disk tests.

Our previous work [2–6] has shown a low coefficient of friction of CuO/3Y-TZP composite when sliding against alumina, but the mechanism of friction reduction was not yet fully understood at that stage. The purpose of this paper is to investigate the mechanism of the friction reduction effect observed in the CuO/3Y-TZP composite against alumina system. In the present study, further pin-on-disk tribological tests for CuO/3Y-TZP composite have been conducted under various conditions. Analysis equipment such as interference microscope, X-ray photoelectron spectroscopy (XPS), micro-Fourier transform infrared spectroscopy (FTIR) and energy dispersive X-ray spectroscopy (EDX) have been used to characterize

* Corresponding authors. Fax: +31 53 489 4784.
E-mail addresses: jiupeng.song@hotmail.com (J. Song), m.valefi@ctw.utwente.nl (M. Valefi).

0043-1648/$ – see front matter © 2011 Elsevier B.V. All rights reserved.
doi:10.1016/j.wear.2011.08.016

the worn surfaces. Combining the results from the different methods gives a good explanation for the low coefficient of friction of CuO/3Y-TZP composite sliding against alumina.

2. Experimental procedure

2.1. Sample preparation

The ceramic disks used for pin-on-disk tribological tests were prepared from commercial available 3Y-TZP (TZ-3Y, Tosoh, Japan) and CuO powder (Alfa Aesar, Germany). The particle size of 3Y-TZP powder was calculated to be approximately 64 nm based on surface area. The particle size of CuO is smaller than 74 μm. A powder mixture of 3Y-TZP with CuO was prepared by ball milling in ethanol for 24 h, using zirconia (ZrO_2) balls as milling medium. The doping level was chosen as 8 mol% (5 wt.%). The milled slurry was oven-dried at 80 °C for 24 h and subsequently at 120 °C for 8 h. The dry cake was then ground slightly in a mortar and sieved through a 180 μm sieve. The powder was shaped in disks with a diameter equal to 50 mm by uniaxial pressing at 5 MPa for 3 min. Each pressured disk was around 23 g and the thickness was about 5 mm. The cold isostatic pressing was employed for the disks subsequently at 400 MPa for 4 min. The densification behavior of the CuO/3Y-TZP composite and pure 3Y-TZP was investigated by a dilatometer [4]. The disks were then sintered in stagnant air at 1500 °C for 8 h. Both heating and cooling rate were 2 °C/min. The sintered samples were ground by a diamond disk and then polished by diamond paste with the particle size of 8 μm. The polished samples were ultrasonically cleaned in ethanol and then annealed at 850 °C for 2 h to remove the residual stress. Heating and cooling rates for annealing were also 2 °C/min.

Pure 3Y-TZP samples were also prepared for the purpose of comparison. The pressing and sintering procedure was the same as above, but the holding time for sintering was reduced to 2 h.

2.2. Sample characterization

The density of sintered disks was measured by the Archimedes method in mercury. The phases of the polished samples were analyzed by X-ray diffraction (XRD) (Philips X'Pert, The Netherlands). A scanning electron microscope (SEM) (Zeiss 1550, Germany) equipped with EDX (Thermo Noran, USA) was used to analyze the as-sintered surfaces and fractured surfaces of the samples. The hardness of the polished samples was measured by an ultra micro hardness tester (Shimadazu DUH-200 Dynamic, Japan) with a Vickers indenter. The maximum indentation force was 2 N, the loading speed was 0.014 N/s, and the holding time at the maximum force was 5 s. For each sintered sample, 10 positions were chosen to measure the hardness. The fracture toughness was obtained using an indentation-strength method with the equation given by Anstis et al. [7]. The applied load for indentation was 98 N and the indentation time was 10 s.

2.3. Tribological tests

Dry sliding tests were performed on a pin-on-disk tribometer (CSM, Switzerland). Commercial available alumina (Al_2O_3), silicon carbide (SiC) and ZrO_2 ceramic balls (Gimex Technische Keramiek B.V., The Netherlands) and AISI-52100 steel balls were used as pin. The main thermal and mechanical properties of the balls were provided by the supplier and the center line average (CLA) surface roughness was measured by the interference microscope (Micromap 512, Micromap Corporation, Germany), as presented in Table 1. The measurement area was 534 μm × 400 μm and the surface heights were measured over 640 × 480 pixels. The diameter of the ceramic balls was 10 mm. The CLA surface roughness

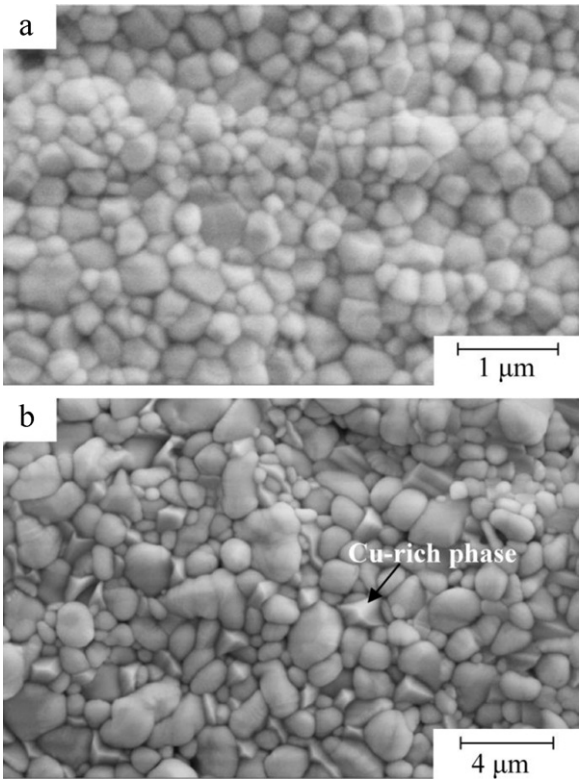

Fig. 1. Scanning electron microscopy images of as-sintered surfaces of (a) pure 3Y-TZP and (b) CuO/3Y-TZP composite.

of the polished CuO/3Y-TZP composite and pure 3Y-TZP disks was approximately 50 nm. The environmental conditions were controlled during the tribological tests at a constant temperature of 23 °C and a relative humidity (RH) of 40%. The normal load on the pin was 1 N and 5 N (maximum, initial, Hertzian contact pressure of 0.4 GPa and 0.9 GPa) and a sliding velocity of 0.1 m/s was used. The sliding distances ranged from 100 m to 5 km to investigate the worn surfaces in both the mild and severe wear regime. The radius of the wear tracks changed from 5 mm to 14 mm. To study the effect of environment, several experiments were conducted in air with various relative humidity level.

Interference microscopy was used to analyze the wear tracks of the discs and wear scars on the balls. The microstructure and chemical composition of the wear tracks was investigated using SEM/EDX (HR-LEO 1550 FEF SEM) and micro-FTIR (FTS-575C equipped with UMA 500 microscope). The chemical contents of the worn surfaces were analyzed by XPS (Quantera SXM, Physical Electronics, USA, using Al K_α (1486.6 Ev) excitation source). The X-ray beam size used in the analysis was 100 μm.

3. Results

3.1. Sample properties

The relative density of the sintered 3Y-TZP disks and the ones doped with 8 mol% CuO are 99.5% and >95% respectively using the theoretical density of 3Y-TZP (6.08 g/cm^3) in all cases. The microstructure of the sintered samples is shown in Fig. 1. The grain size for CuO/3Y-TZP composite is 2 μm and for pure 3Y-TZP is 450 nm. The copper rich grains of the CuO/3Y-TZP composite are identified by EDX and characterized as the brighter and angular grains see Fig. 1. It is shown by Ran et al. [4] that a copper rich grain boundary phase as well as small CuO crystalline grains are formed

Table 1
Parameters for the balls (diameter 10 mm) used in the pin-on-disk tribological tests.

Material	Hardness (GPa)	Elastic modulus (GPa)	Bending strength (MPa)	Thermal conductivity (W/m K)	CLA surface roughness (nm)
Al_2O_3	20	320	340	29	31.2
SiC	25	430	420	110	4.4
Y_2O_3–ZrO_2	13	205	1000	2	6.0
Steel	7.55	213	750	46	9.0

when 5 wt.% CuO added to 3Y-TZP The details of phase analysis and microstructure are discussed elsewhere [4].

The average hardness of 3Y-TZP is 13 GPa and the standard deviation is 0.4 GPa. The hardness of CuO/3Y-TZP composite sample is lower and less homogeneous. The measured micro hardness has an average value of 9.5 GPa with a standard deviation of 1 GPa. The fracture toughness K_{IC} for the CuO/3Y-TZP composite and pure 3Y-TZP samples is 3.5 ± 0.2 MPa $m^{1/2}$ and 4.2 ± 0.2 MPa $m^{1/2}$ respectively and has been measured by indentation.

3.2. Friction behavior

The pin-on-disk tribological tests using a low normal load of 1 N presented in Fig. 2 show an evident friction reduction effect by adding 3Y-TZP with CuO. The coefficient of friction for pure 3Y-TZP disk sliding against Al_2O_3 pin is 0.46 after a sliding distance of 5 km (6.63×10^4 sliding passes). The CuO/3Y-TZP composite shows a low coefficient of friction of 0.19 under the same test conditions. As the normal load increases to 5 N, the region with low friction reduces to approximately 1 km (1.72×10^4 sliding passes). There is an abrupt jump in the coefficient of friction after this period (see Fig. 3). During the low friction region, the friction coefficient reduces from 0.76 to 0.30 by the addition of 8 mol% CuO in the 3Y-TZP. However, this friction reduction is not the intrinsic characteristic of the addition of CuO to 3Y-TZP but it is a combination CuO addition to 3Y-TZP and Al_2O_3 as counter material. Clearly there is no evident friction reduction effect when sliding against SiC, ZrO_2 or steel balls, as shown in Table 2. Pasaribu et al. [5] investigated the humidity effect on the friction behavior for the pure 3Y-TZP and CuO/3Y-TZP composite. The experimental results show that the friction reduction by the addition of CuO is not observed at relative humidity of 15%. From the results as indicated in Fig. 4 one can conclude that some water is necessary for friction reduction in Al_2O_3 and CuO/3Y-TZP composite couples.

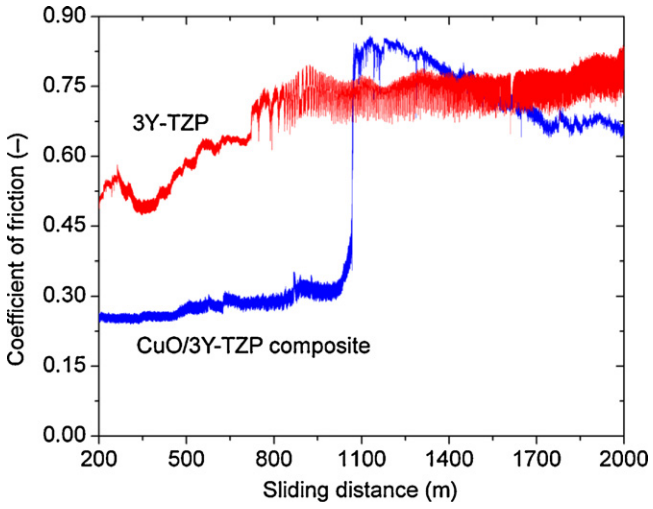

Fig. 3. Transition of friction from low to high region for CuO/3Y-TZP composite sliding against Al_2O_3 pins (normal load 5 N, sliding velocity 0.1 m/s, relative humidity 40%, 23 °C).

Table 2
Coefficient of friction after 1 km sliding distance of pure 3Y-TZP and CuO/3Y-TZP composite against pins of various materials (normal load 5 N, sliding velocity 0.1 m/s, relative humidity 40%, 23 °C).

Pins	Disk	
	3Y-TZP	CuO/3Y-TZP
SiC	0.52	0.50
ZrO_2	0.73	0.80
Steel	0.63	0.70
Al_2O_3	0.72	0.30

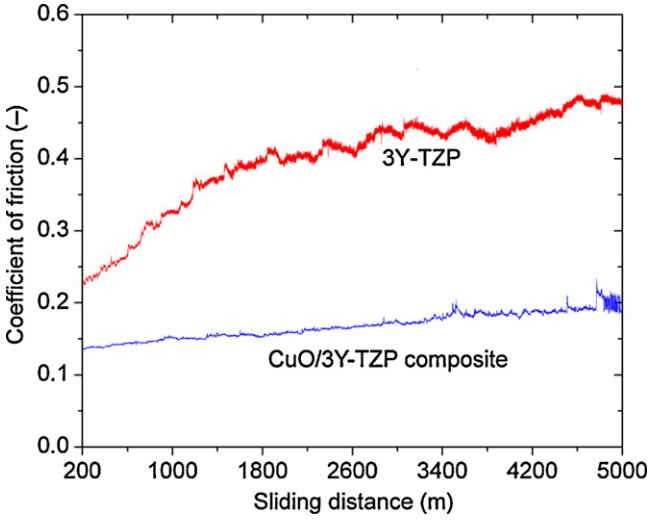

Fig. 2. Low coefficient of friction for pure 3Y-TZP and CuO/3Y-TZP composite sliding against Al_2O_3 pins (normal load 1 N, sliding velocity 0.1 m/s, relative humidity 40%, 23 °C).

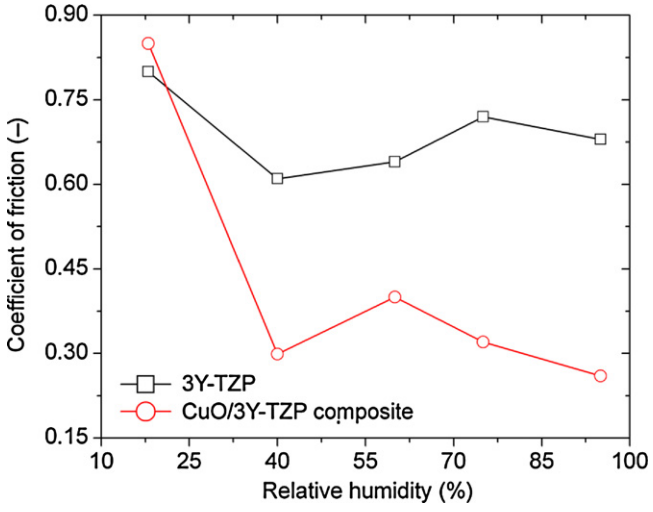

Fig. 4. Coefficients of friction after the running-in stage for pure 3Y-TZP and CuO/3Y-TZP composite sliding against Al_2O_3 pins under various relative humidity conditions (normal load 5 N, sliding velocity 0.1 m/s, 23 °C).

Table 3
Coefficient of friction after running-in, i.e. steady state, of pure 3Y-TZP and CuO/3Y-TZP composite against Al_2O_3 (normal load 5 N, sliding velocity 0.1 m/s, relative humidity 40%, 23 °C).

Sliding distances	Coefficient of friction	
	3Y-TZP	CuO/3Y-TZP
100 m	0.57	0.33
200 m	0.47	0.27
500 m	0.67	0.30
850 m	0.55	0.51
1000 m	0.70	0.81

3.3. Wear behavior

In order to understand the mechanism of friction reduction of CuO/3Y-TZP when sliding against an Al_2O_3 pin, the wear tracks of the disks and the wear scar of the balls have been investigated. The wear tracks after a sliding distance of 100 m (3174 sliding passes), 200 m (4545 sliding passes), 500 m (8821 sliding passes), 850 m (13470 sliding passes) and 1000 m (13252 sliding passes) for both CuO/3Y-TZP composite and pure 3Y-TZP disks were analyzed by using interference microscopy. The normal load of 5 N, the sliding velocity of 0.1 m/s and the relative humidity of 40% were kept constant during these tribological tests. The coefficient of friction after running-in, i.e. steady-state, is shown in Table 3. For the CuO/3Y-TZP composite, the wear tracks with a sliding distance of 100 m, 200 m and 500 m show a low coefficient of friction and mild wear. The coefficient of friction for a sliding distance of 850 m and beyond is high and the wear is severe.

The profiles of the wear tracks for the CuO/3Y-TZP composite measured by interference microscopy are shown in Fig. 5. The wear tracks (a)–(c) related to low friction are smooth. There is a thin layer with a thickness of less than 200 nm on the worn surface due to wear debris, measured by interference microscope [8,9]. This results in wear tracks elevated above the sample surface. The wear track (d) corresponding to the transition of the low coefficient of friction to the high friction level becomes rough. Wear increases and more wear debris is collected on the wear tracks. The non-uniform layer on the worn surface becomes thicker than 500 nm. For pure 3Y-TZP in Fig. 6, the wear tracks (a) and (b) are smooth and there is a very small amount of wear debris on the worn surface. However, after the sliding distance is more than 500 m, ploughing occurs and results in a rough wear track.

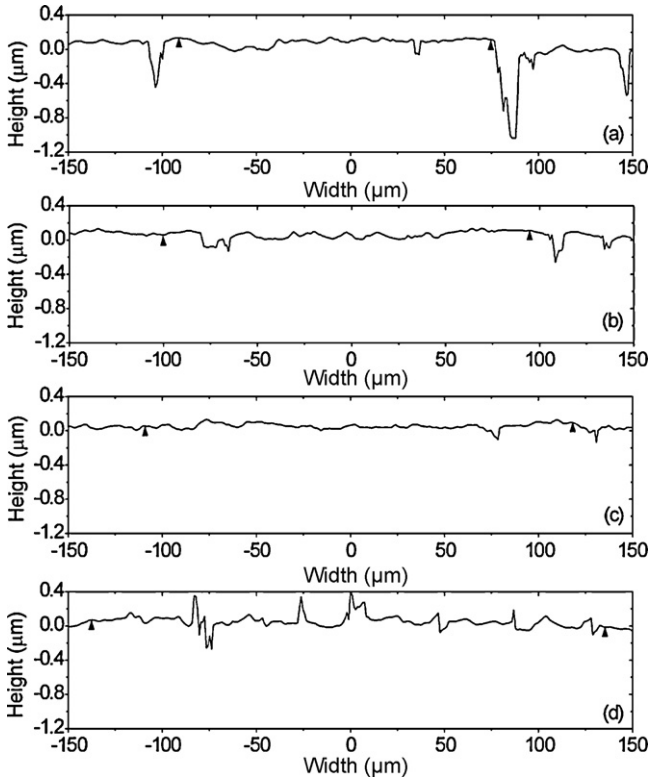

Fig. 5. Profiles of the wear tracks for CuO/3Y-TZP composite sliding against Al_2O_3 for various sliding distances: (a) 100 m, (b) 200 m, (c) 500 m and (d) 850 m (normal load 5 N, sliding velocity 0.1 m/s, relative humidity 40%, 23 °C). The distance between arrows indicates the width of the track.

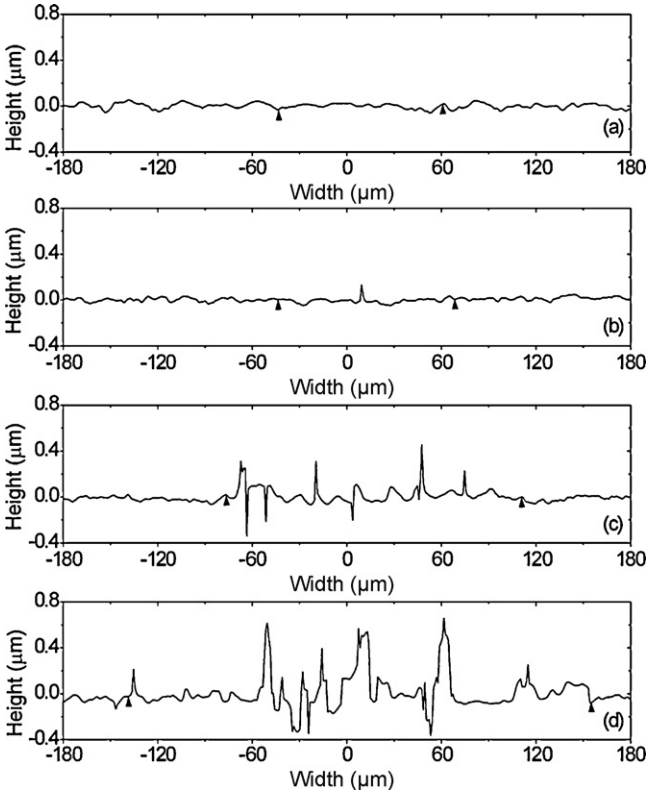

Fig. 6. Profiles of the wear tracks for pure 3Y-TZP sliding against Al_2O_3 for various sliding distances: (a) 100 m, (b) 200 m, (c) 500 m and (d) 850 m (normal load 5 N, sliding velocity 0.1 m/s, relative humidity 40%, 23 °C). The distance between arrows indicates the width of the track.

The wear tracks are covered with a layer formed by wear debris and it is not easy to measure neither the wear volume nor weight loss of the disk. The wear volume for the balls can be analyzed by interference microscopy (see Fig. 7). For a sliding distance of 100 m or 200 m, the coefficient of friction for an Al_2O_3 pin sliding against CuO/3Y-TZP composite disc is lower than against pure 3Y-TZP. Furthermore, the wear volume of the Al_2O_3 pin is higher when it is sliding against CuO/3Y-TZP disk. After the transition of a low friction coefficient to the high friction region for CuO/3Y-TZP at a sliding distance of 850 m, the wear for both ball and disk increases abruptly. The calculated wear rates of the Al_2O_3 pins are given in Table 4.

3.4. Analysis by XPS

XPS analysis results as given in Table 5 show that the fractured surface of CuO/3Y-TZP has approximately two times more Cu than the surface. This means that most Cu distributes on the grain boundaries and fracture occurs along the grain boundaries due to the low strength and grain boundary weakening. The wear tracks with a sliding distance of 200 m, 500 m, 850 m and 1000 m as described

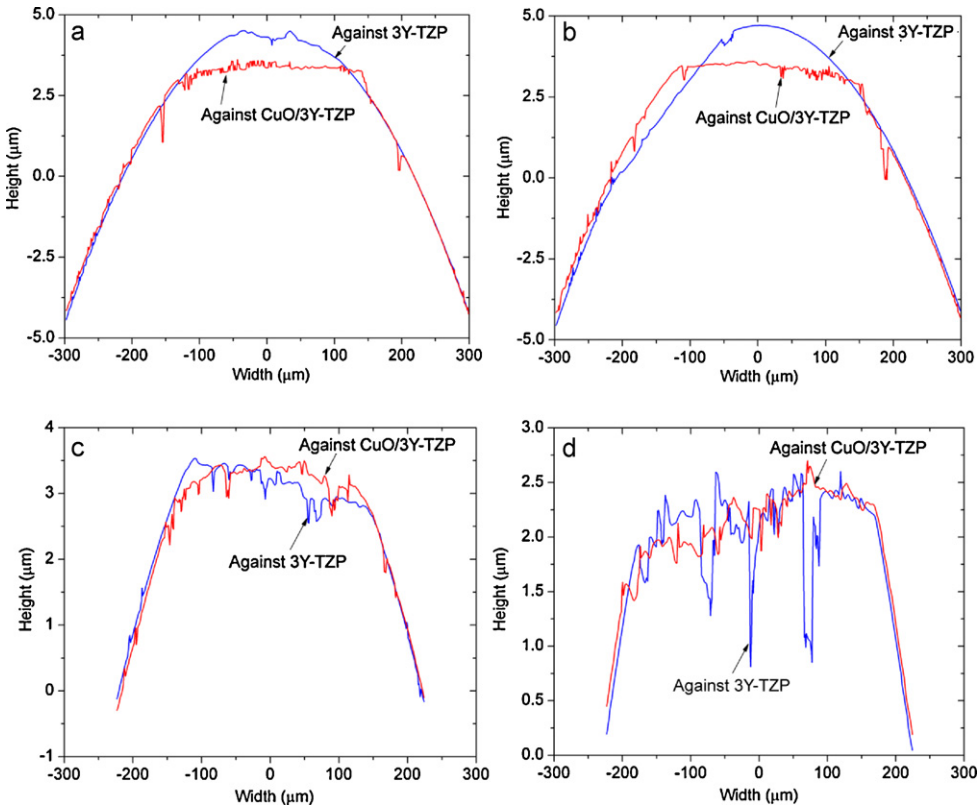

Fig. 7. Wear profiles of Al_2O_3 pins after sliding tests against pure 3Y-TZP and CuO/3Y-TZP composite with sliding distances: (a) 100 m, (b) 200 m, (c) 500 m and (d) 850 m (normal load 5 N, sliding velocity 0.1 m/s, relative humidity 40%, 23 °C).

Table 4
Wear rates of Al_2O_3 pins after certain sliding distances against pure 3Y-TZP and CuO/3Y-TZP composite against (normal load 5 N, sliding velocity 0.1 m/s, relative humidity 40%, 23 °C).

Sliding distances	Wear rates ($\times 10^{-7}$ mm^3/(N m))	
	3Y-TZP	CuO/3Y-TZP
100 m	0.6	5.2
200 m	0.7	5.1
500 m	1	0.9
850 m	2.1	4.1

above are analyzed by XPS. The elemental composition on the wear tracks of CuO/3Y-TZP sliding against an Al_2O_3 pin is given in Table 6. If the atomic ratios of Al/Zr are chosen to analyze the chemical components of the wear debris compacted on the surfaces, Al/Zr is 37.4% (standard deviation of 3.5%) for the wear track with sliding distance of 200 m. For the wear track with sliding distance of 500 m, Al/Zr is 41.5% (standard deviation of 12.7%). The Al content reduces after the transition to high friction region. Al/Zr is 23.3% (standard deviation of 4.6%) for the wear track with sliding distance of 850 m. The one

Table 5
Elemental composition of fractured and polished surfaces of the CuO/3Y-TZP composite analyzed by XPS.

Measured surfaces	Atomic % metallic elements		
	Cu(2p3)	Y(3d)	Zr(3d)
Polished			
Mean	6.98	7.10	85.92
Standard deviation	1.07	0.53	1.23
Fractured			
Mean	16.24	9.14	74.61
Standard deviation	1.68	1.45	1.01

for the wear track with the sliding distance of 1000 m is 19.4% (standard deviation of 1.6%). The Cu content on the worn surface is not homogeneous and has no evident relation with sliding distance i.e. friction and wear. The ratio of Y/Zr is approximately homogeneous and ranges from 4.59% to 6.76% for various wear tracks.

3.5. *Microstructural and compositional analysis by SEM/EDX and micro-FTIR*

The microstructure of the wear track of pure 3Y-TZP and CuO/3Y-TZP composite against Al_2O_3 pin with a sliding distance of 100 m is shown in Fig. 8. Both wear tracks are in the mild wear region and the width of the wear track is approximately 150 μm. The surfaces of both wear tracks are smooth, but the coefficient of friction is different. The coefficients of friction for the pure

Table 6
Elemental composition of the wear tracks of the CuO/3Y-TZP composite sliding against Al_2O_3 with various sliding distances analyzed by XPS (normal load 5 N, sliding velocity 0.1 m/s, relative humidity 40%, 23 °C).

Sliding distances	Atomic % metallic elements				Atomic ratio (%)	
	Al(2p)	Cu(2p3)	Y(3d)	Zr(3d)	Al/Zr	Cu/Zr
200 m						
Mean	25.07	3.59	3.59	67.75	37.4	5.3
Standard deviation	1.32	1.10	1.10	3.33	3.5	1.2
500 m						
Mean	25.90	10.70	2.94	60.45	41.5	16.1
Standard deviation	6.13	8.40	1.68	12.25	12.7	9.6
850 m						
Mean	17.62	2.18	4.69	75.51	23.3	2.9
Standard deviation	0.89	0.95	0.75	0.90	4.6	10.5
1000 m						
Mean	15.00	2.44	5.24	77.34	19.4	3.1
Standard deviation	1.40	0.39	0.25	1.19	1.6	0.4

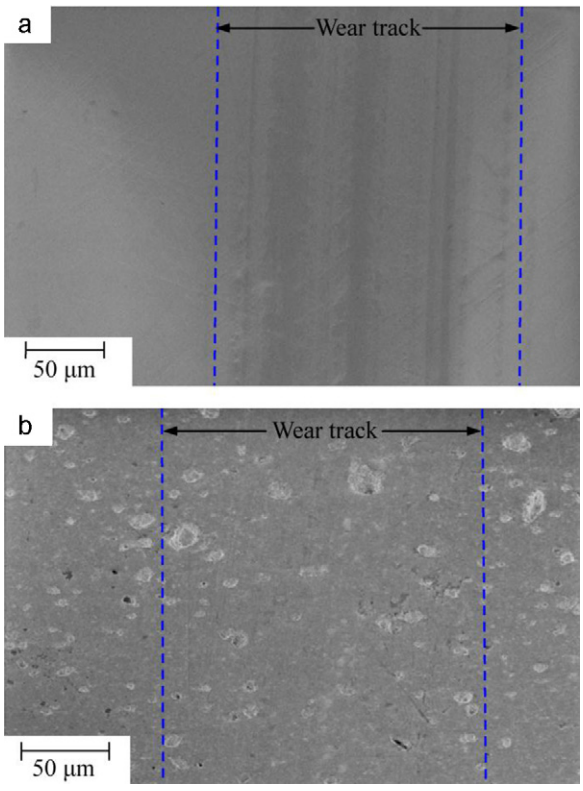

Fig. 8. Scanning electron microscopy images of the wear tracks of (a) pure 3Y-TZP and (b) CuO/3Y-TZP composite sliding against Al_2O_3 at a sliding distance of 100 m (normal load 5 N, sliding velocity 0.1 m/s, relative humidity 40%, 23 °C).

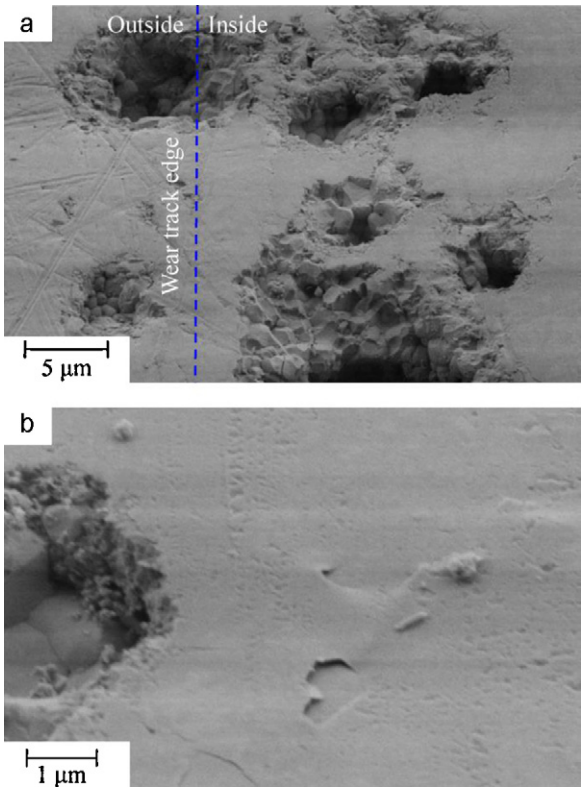

Fig. 9. Scanning electron microscopy images of the surface layer on the wear tracks of CuO/3Y-TZP composite sliding against Al_2O_3 pin at a sliding distance of 100 m: (a) wear track edge and (b) inside wear track (normal load 5 N, sliding velocity 0.1 m/s, relative humidity 40%, 23 °C).

3Y-TZP and CuO/3Y-TZP composite are 0.57 and 0.33 respectively. The low coefficient of friction for CuO/3Y-TZP can be attributed to the patched layer on the wear track, as shown in Fig. 9. The scratches due to polishing are clearly visible outside the wear track in Fig. 9(a), but inside the wear track they are covered by the layer. It is clearly visible that most of the layers are formed around the holes inside the wear track. The thickness of the layer shown in Fig. 9(b) is less than 200 nm. Nanoindentation tests show that this layer is much softer compared to the substrate and as a consequence a friction reduction is observed [3]. The SEM backscatter-mode image in Fig. 10(a) shows the patched layer (dark region II) is a different material compared to the other regions of the wear track (light region I). The comparison of EDX analysis, shown in Fig. 10(b) and (c), proves that the patched layer (dark region II) is an Al-rich material.

After the coefficient of friction jumps to the high value for CuO/3Y-TZP sliding against the Al_2O_3 pin, the wear track becomes rough and a large amount of grain pull-out wear debris is collected on the surface (see Fig. 11(a) and (b)). Due to the increased wear of the CuO/3Y-TZP disk, the Al content in the wear debris on the surface is reduced by comparison with the mild wear track, as shown by the EDX analysis results in Fig. 11(c). Intergranular fracture is observed in the severe wear track (see Fig. 12). Some grains are pulled out in the same wear track (see Fig. 13).

To further analyze the chemical composition of the patchy layer, micro-FTIR has been performed at different spots: inside the wear track, outside the wear track and the wear debris formed after the transition from mild to severe. Since the amount of wear debris before transition was very small, the wear debris collected for analysis were after the transition in friction. Fig. 14 shows the micro-FTIR spectra at three different positions. All spectra show a strong peak at 823 cm^{-1}. Gee [10] reported a similar peak at 840 cm^{-1} inside the wear track while the formation of aluminum hydroxide during wear of alumina was studied. The broad peak at about 3300 cm^{-1} signifies the presence of hydroxide in the wear debris as reported by other researchers [11–13]. Since the wear debris collected at the early stage of the wear transition, it would be expected a thin hydroxide surface film was also present at wear track. This is in good agreement with literature, which shows formation of aluminum hydroxide is responsible for friction reduction [11].

4. Discussion

Our previous work has analyzed the friction reduction effect of CuO/3Y-TZP composite sliding against alumina and it concluded that this was due to the formation of a soft layer formed on the hard substrate [9]. The interference microscope analysis on the wear track profile in Fig. 7 and the SEM images in Fig. 9 show that a non-uniform surface layer with a thickness less than 200 nm is formed on the mild wear track of CuO/3Y-TZP composite sliding against Al_2O_3. Nanoindentation tests have proven that this layer is much softer than the substrate [3]. However, the formation of this layer depends on many factors such as the addition of CuO, counterbody material and humidity.

The low friction has only been found when the CuO/3Y-TZP composite disk is sliding against an Al_2O_3 pin. There is no friction reduction found for the ZrO_2, SiC and steel pins sliding against the CuO/3Y-TZP composite. Further it is found that at low relative humidity (15%), the friction for the CuO/3Y-TZP composite is also high (see Fig. 4). The high Al content on the wear track surfaces with low friction, as analyzed by XPS, indicates that the debris layer mainly comes from the Al_2O_3 counterface. Furthermore micro-FTIR shows that this wear debris mainly composes of hydroxide. Al_2O_3 can react with moisture under high local contact

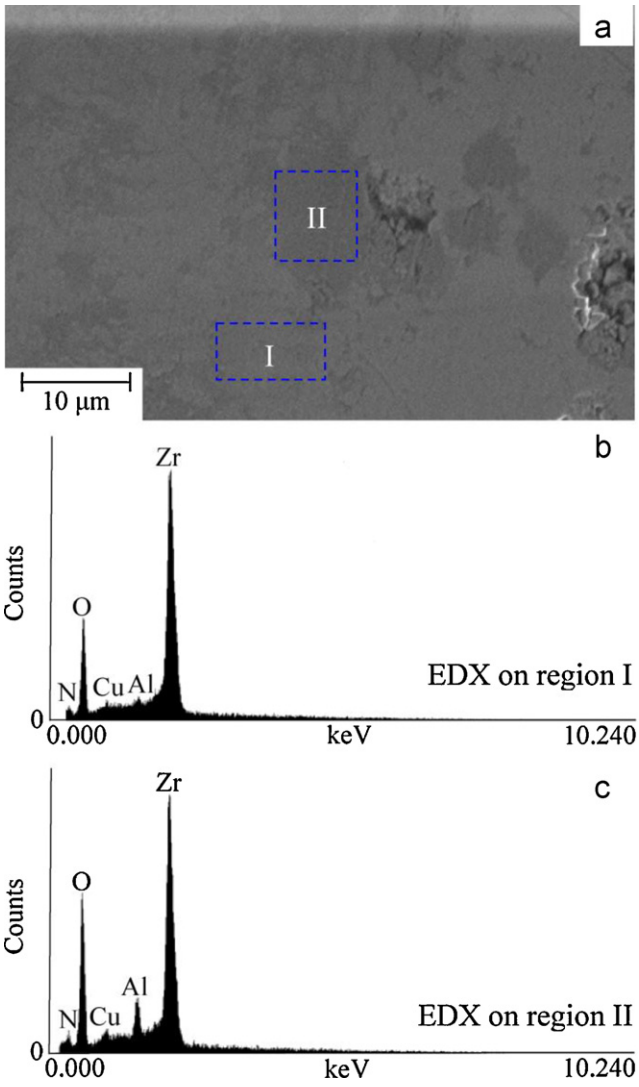

Fig. 10. (a) Backscatter-mode scanning electron microscopy image of the mild wear track of CuO/3Y-TZP composite sliding against Al_2O_3 at a sliding distance of 100 m (normal load 5 N, sliding velocity 0.1 m/s, relative humidity 40%, 23 °C). The energy-dispersive X-ray analysis is for (b) light region I and (c) dark region II in (a).

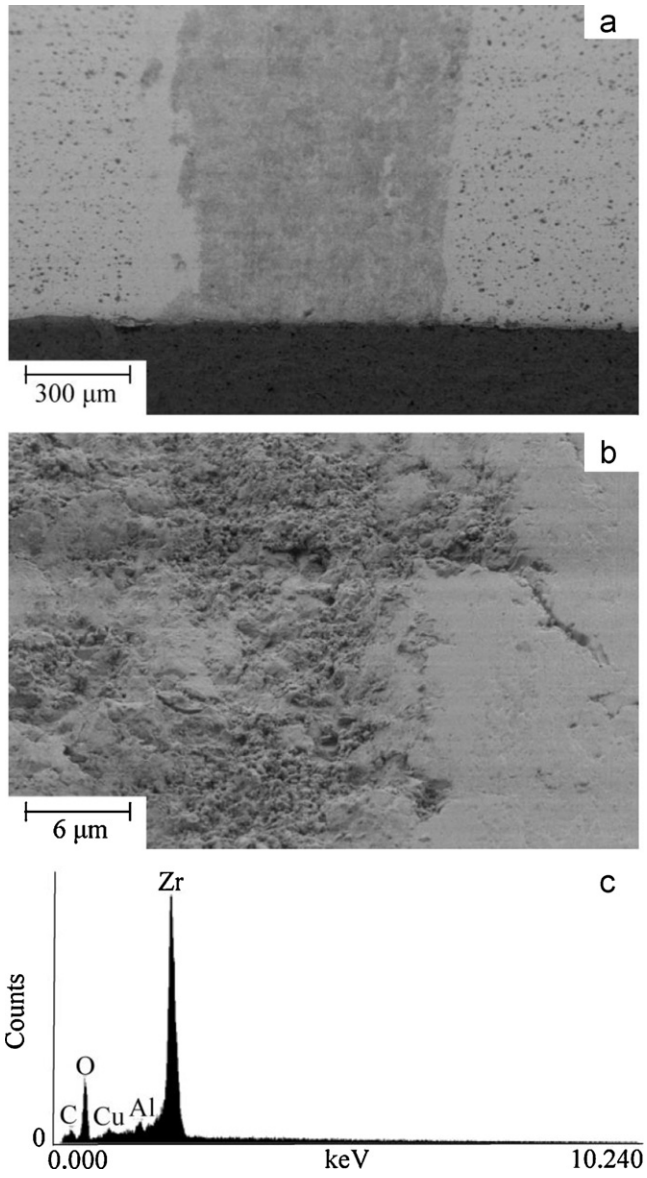

Fig. 11. Scanning electron microscopy image of the severe wear track of CuO/3Y-TZP composite sliding against Al_2O_3 at a sliding distance of 1000 m (normal load 5 N, sliding velocity 0.1 m/s, relative humidity 40%, 23 °C): (a) with low magnification and (b) with high magnification inside the wear track. The energy-dispersive X-ray analysis (c) is for the wear track region in (b).

pressures and temperatures to form aluminum hydroxide [13]. It has been reported that aluminum hydroxide has a layered crystallographic structure, which is expected to offer friction reducing properties [14,15]. Although the formation mechanism is not completely clear, it is likely that the hydroxide is indirectly formed by reaction of alumina wear debris with water. This is because very tiny Al_2O_3 debris particles have been generated during the wear process of Al_2O_3. Particle sizes as low as 20 nm in size are observed by XRD and transmission electron microscopy (TEM) observations [13]. This very fine Al_2O_3 debris is forced into any depressions in the surface and the reaction of Al_2O_3 wear debris to form hydroxide takes place. This process continues until a hydroxide film is formed on, resulting in a very smooth surface [16].

Based on the different tribological behavior between pure 3Y-TZP and CuO/3Y-TZP composite against Al_2O_3 investigated above, it can be concluded CuO plays an important role in the formation of the soft surface layer. In the low friction region, the wear rate of the Al_2O_3 pin is a few times higher when compared to sliding against pure 3Y-TZP (see Table 4; see also Fig. 7(a) and (b)). So for the CuO/3Y-TZP composite, Al_2O_3 debris supplied in a proper quantity to form the aluminum hydroxide layer. It has been reported that the wear mechanism in TZP is plastic deformation and delamination [17]. This can retard the formation of wear debris by micro fracture which further enhances the wear of the alumina ball. For the CuO/3Y-TZP composite material this wear mechanism will be less. XRD results which show that CuO/3Y-TZP composite contain 70% monoclinic phase, while 3Y-TZP has 100% tetragonal phase after polishing and heat treatment. The absence of tetragonal to monoclinic phase transformation in CuO/3Y-TZP composite is responsible for micro fracture or micro chipping and wear of CuO/3Y-TZP composite at the beginning of a friction test. It is most likely that the wear debris is entrapped at the interface and causes more wear of the alumina ball. Further, CuO can react with alumina to form the phase $CuAl_2O_4$ or $CuAlO_2$ [18]. Reaction of alumina and CuO has been studied and it shows negative free energy of reaction which means that this reaction is highly favored [19]. For the CuO-α-Al_2O_3 system, it is known that CuO debris decomposes to Cu_2O by mechanical activation [20]. This Cu_2O further reacts with α-Al_2O_3 to form $CuAlO_2$. Further, it has been found that the alternative oxide $CuAl_2O_4$ oxide is not favored [21,22]. The compound

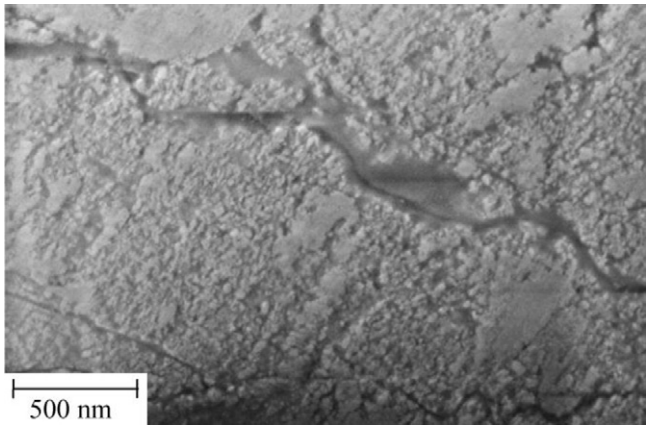

Fig. 12. Scanning electron microscopy image of the intergranular fracture in the severe wear track of CuO/3Y-TZP composite sliding against Al_2O_3 at a sliding distance of 1000 m (normal load 5 N, sliding velocity 0.1 m/s, relative humidity 40%, 23 °C).

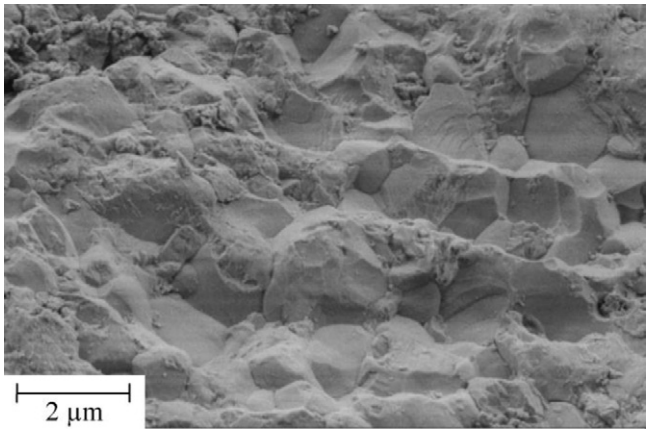

Fig. 13. Scanning electron microscopy image of the pulling out of grains in the severe wear track of CuO/3Y-TZP composite sliding against Al_2O_3 at a sliding distance of 1000 m (normal load 5 N, sliding velocity 0.1 m/s, relative humidity 40%, 23 °C).

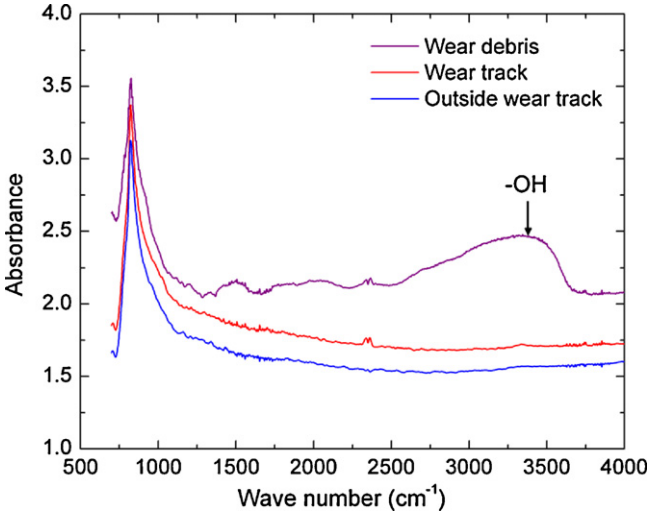

Fig. 14. Micro-FTIR spectrums on the surface of CuO/3Y-TZP composite disc at room temperature.

$CuAlO_2$ was also detected in the present material by XRD measurement on the contact surface of CuO/3Y-TZP composite sliding against Al_2O_3 when CuO is higher than 5 wt.% [2].

Further, Pepper [23] performed pin-on-disk experiments using Al_2O_3 pin with metallic disks of Cu, Ni or Fe. When the tests were performed in O_2, friction for using the Cu disk was lower than that for the Ni or Fe disk. During sliding the complex oxides $CuAlO_2$, $NiAl_2O_4$ and $FeAl_2O_4$ were formed by chemical reactions between metal oxides and Al_2O_3. Among these oxides, only $CuAlO_2$ reduced the friction.

Based on the above discussion, it is suggested that the formation of aluminum hydroxide as well as $CuAlO_2$ provide a low shear strength interface which results in low friction. Copper oxide not only enhances formation of aluminum hydroxide but also contributes to the formation of $CuAlO_2$, which also reduces friction.

5. Conclusions

Referring to our previous work on the tribological properties of the CuO/3Y-TZP composite, the mechanism of friction reduction of this material sliding against Al_2O_3 has been investigated and attributed to the formation of an Al-rich soft layer on the contact surface. It is found out that counter body material of Al_2O_3 and humidity are important for obtaining low friction during sliding tests. This surface layer is less than 200 nm thick during the low friction region. The micro chipping in the mild wear region produces very fine wear debris of Al_2O_3 and this debris can react with water to form aluminum hydroxide. The soft aluminum hydroxide is compacted on the contact surface makes the surface smooth, which reduces the friction. In addition, formation of $CuAlO_2$ with low shear strength at interface results in lower friction. CuO not only enhances formation of aluminum hydroxide but also contributes in the formation of $CuAlO_2$. The sliding distance characterized with a low coefficient of friction is sensitive to the applied normal load (contact pressure). At the end of this stage, the coefficient of friction jumps to a high value abruptly because the wear mechanism changes from micro chipping to intergranular fracture.

Acknowledgements

Funding of this work was supported by the Dutch governmental program IOP Self Healing Materials. The authors would like to thank E.G. de Vries and W. Lette for tribological tests and T. Bor and C. Padberg for XRD and micro-FTIR analysis.

References

[1] H. Liu, Q. Xue, The tribological properties of TZP-graphite self-lubricating ceramics, Wear 198 (1996) 143–149.
[2] B. Kerkwijk, M. Garćýa, W.E. van Zyl, L. Winnubst, E.J. Mulder, D.J. Schipper, H. Verweij, Friction behaviour of solid oxide lubricants as second phase in α-Al_2O_3 and stabilized ZrO_2 composites, Wear 256 (2004) 182–189.
[3] H.R. Pasaribu, J.W. Sloetjes, D.J. Schipper, Friction reduction by adding copper oxide into alumina and zirconia ceramics, Wear 255 (2003) 699–707.
[4] S. Ran, L. Winnubst, D.H.A. Blank, H.R. Pasaribu, J.W. Sloetjes, D.J. Schipper, Effect of microstructure on the tribological and mechanical properties off CuO-doped 3Y-TZP ceramics, J. Am. Ceram. Soc. 90 (9) (2007) 2747–2752.
[5] H.R. Pasaribu, K.M. Reuver, D.J. Schipper, S. Ran, K.W. Wiratha, A.J.A. Winnubst, D.H.A. Blank, Environmental effects on friction and wear of dry sliding zirconia and alumina ceramics doped with copper oxide, Int. J. Refract. Met. Hard Mater. 23 (2005) 386–390.
[6] .E. Tocha, H.R. Pasaribu, D.J. Schipper, H. Schönherr, G.J. Vancso, Low friction in CuO-doped yttria-stabilized tetragonal zirconia ceramics: a complementary macro- and nanotribolology study, J. Am. Ceram. Soc. 91 (5) (2008) 1646–1652.
[7] G.R. Anstis, P. Chantikul, B.R. Lawn, D. Marshall, A critical evaluation of indentation techniques for measuring fracture toughness: I, direct crack measurements, J. Am. Ceram. Soc. 64 (9) (1981) 533–538.
[8] H.R. Pasaribu, Friction and wear of zirconia and alumina ceramics doped with CuO, Ph.D. Thesis, University of Twente, Enschede, The Netherlands, 2005.

[9] H.R. Pasaribu, D.J. Schipper, Deterministic friction model of a rough surface sliding against a flat layered surface, Tribol. Lett. 17 (4) (2004) 967–976.
[10] M.G. Gee, The formation of aluminum hydroxide in the sliding wear of alumina, Wear 153 (1992) 201–227.
[11] X. Dong, S. Jahanmir, S.M. Hsu, Tribological characteristics of α-alumina at elevated temperatures, J. Am. Ceram. Soc. 74 (5) (1991) 1036–1044.
[12] R.J. Mortimer, R.J. Mayes, Characterisation and humidity-sensing properties of aluminium (oxy)-hydroxide films prepared by cathodically induced precipitation, Sens. Actuators B 128 (2007) 124–132.
[13] M.G. Gee, E.A. Almond, The effect of surface finish on the wear of alumina, J. Mater. Sci. 25 (1990) 296–310.
[14] K. Wefer, G.M. Bell, Oxides and Hydroxides of the Aluminum, Technical Paper 19, Alcoa Research Laboratories, 1972.
[15] C. Misra, Industrial Alumina Chemicals, American Chemical Society, 1986, 17.
[16] O.O. Ajayi, K.C. Ludema, Mechanism of transfer film formation during repeat pass sliding of ceramic materials, Wear 140 (1990) 191–206.
[17] Y. He, L. Winnubst, A.J. Burggraaf, H. Verweij, P.G. Van der Vast, B. de With, Grain-size dependence of sliding wear in tetragonal zirconia polycrystals, J. Am. Ceram. Soc. 79 (1996) 3090–3096.
[18] S.K. Misra, A.C.D. Chaklader, The system copper oxide–alumina, J. Am. Ceram. Soc. 46 (10) (1963) 509.
[19] M. Gadalla, J. White, Equilibrium relationships in the system Cu_2O–CuO–Al_2O_3, Trans. Br. Ceram. Soc. 563 (1964) 39–62.
[20] K. Tokumitsu, Reduction of metal oxides by mechanical alloying method, Solid State Ionics 101–103 (1997) 25–31.
[21] T. Tsuchida, R. Furuchi, T. Sukegawa, M. Furudate, T. Ishii, Thermoanalytical study on the reaction of the CuO–Al_2O_3(η, γ and α) systems, Thermochim. Acta 78 (1984) 71–80.
[22] K.T. Jacob, C.B. Alcock, Thermodynamics of $CuAlO_2$ and $CuAl_2O_4$ and phase equilibria in the system Cu_2O–CuO–Al_2O_3, J. Am. Ceram. Soc. 58 (1975) 192–195.
[23] S.V. Pepper, Effect of adsorbed films on friction of Al_2O_3–metal systems, J. Appl. Phys. 47 (6) (1976) 2579–2583.